Journal of Medicinal Chemistry

Article

pubs.acs.org/jmc

Antitumor Agent Calixarene 0118 Targets Human Galectin-1 as an Allosteric Inhibitor of Carbohydrate Binding

Ruud P. M. Dings,[†,⊥] Michelle C. Miller,[†,⊥] Irina Nesmelova,[†] Lucile Astorgues-Xerri,[‡] Nigam Kumar,[†] Maria Serova,[§] Xuimei Chen,[∥] Eric Raymond,[‡] Thomas R. Hoye,[∥] and Kevin H. Mayo*[,†]

[†]Department of Biochemistry, Molecular Biology & Biophysics, University of Minnesota Health Sciences Center, 6-155 Jackson Hall, 321 Church Street, Minneapolis, Minnesota 55455, United States

[‡]INSERM U728, and Department of Medical Oncology, Beaujon University Hospital (AP-HP−PRES Paris 7 Diderot), 100 bd du Général Leclerc, 92110 Clichy, France

[§]AAREC Filia Research, 1 place Paul Verlaine, 92100 Boulogne-Billancourt, France

[∥]Department of Chemistry, University of Minnesota, Minneapolis, Minnesota 55455, United States

ABSTRACT: Calix[4]arene compound 0118 is an angiostatic agent that inhibits tumor growth in mice. Although 0118 is a topomimetic of galectin-1-targeting angiostatic amphipathic peptide Anginex, we had yet to prove that 0118 targets galectin-1. Galectin-1 is involved in pathological disorders like tumor endothelial cell adhesion and migration and therefore presents a relevant target for therapeutic intervention against cancer. Here, $^{15}N-^{1}H$ HSQC NMR spectroscopy demonstrates that 0118 indeed targets galectin-1 at a site away from the lectin's carbohydrate binding site and thereby attenuates lactose binding to the lectin. Flow cytometry and agglutination assays show that 0118 attenuates binding of galectin-1 to cell surface glycans, and the inhibition of cell proliferation by 0118 is found to be correlated with the cellular expression of the lectin. In general, our data indicate that 0118 targets galectin-1 as an allosteric inhibitor of glycan/carbohydrate binding. This work contributes to the clinical development of antitumor calixarene compound 0118.

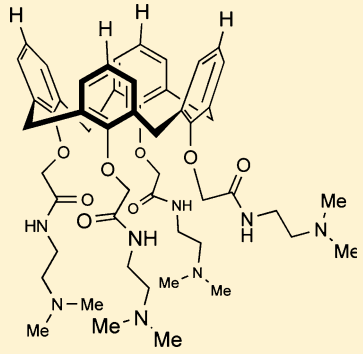

INTRODUCTION

Galectins, which are generally known to bind to β-galactosides at a canonical site in the carbohydrate recognition domain (CRD),[1] exhibit various extracellular activities to mediate cell−cell and cell−matrix adhesion and migration by interacting with various glycan groups of cell surface glycoconjugates.[2] For example, galectin-1 (gal-1) interacts with various glycoconjugates of the extracellular matrix (e.g., laminin, fibronectin, β1 subunit of integrins, and ganglioside GM1), as well as those on endothelial cells (e.g., integrins $\alpha_v\beta_3$ and $\alpha_v\beta_5$, ROBO4, CD36, and CD13)[3] and on T lymphocytes (e.g., CD7, CD43, and CD45), where it is known to induce apoptosis.[4] Binding to cell surface glycoproteins can also trigger intracellular activity, e.g., elements of the Ras-MEK-ERK pathway.[5]

Because antagonists of galectins in general have therapeutic potential as anti-inflammatory[6] and anticancer agents,[7] considerable efforts have been made by many laboratories to design galectin antagonists. To date, reported galectin antagonists are mostly β-galactoside analogues and glycomimetics that target the apparent, canonical β-galactoside carbohydrate binding site.[8−11]

Previously, we reported that the de novo designed peptide 33mer Anginex and its partial peptidomimetic 6DBF7 (see Figure 1) inhibit angiogenesis and tumor growth[12,13] by targeting galectin-1.[14] Using a structure-based design approach, we then designed and synthesized a totally nonpeptidic calix[4]arene-based library of topomimetics of Anginex and 6DBF7.[15] This small calixarene library displays chemical substituents to approximate the molecular dimensions and amphipathic features (hydrophobic and positively charged residues) of Anginex and 6DBF7, which, like many antiangiogenics, consist primarily of amphipathic and cationic antiparallel β-sheet structure as the functional unit.[12] From this topomimetic library, calixarene 0118 (Figure 1) was shown to be a potent angiogenesis inhibitor in vitro, as determined by endothelial cell proliferation, migration, and chick embryo chorioallantoic membrane assays.[15] Calixarene 0118 was also found to be highly effective at inhibiting tumor angiogenesis and tumor growth in murine tumor models (i.e., MA148 human ovarian carcinoma and B16 murine melanoma).[15] In addition, Anginex and 0118 both display multimodal activities, i.e., inhibition of EC proliferation and promotion of leukocyte infiltration into tumors.[16] Such multimodal activities would have advantages in the clinic by, e.g., (i) preventing tumor angiogenesis and inducing vessel normalization,[17] (ii) abrogating tumor escape from immunity through blockade of gal-1-induced apoptosis in activated T lymphocytes,[16,18] and (iii) preventing metastasis formation through inhibition of galectin-1 facilitated tumor cell-EC interactions.[19]

Although Anginex and 0118 function similarly, we had no evidence that 0118 targeted gal-1, as does Anginex. In the

Received: January 4, 2012
Published: May 10, 2012

dx.doi.org/10.1021/jm300014q | J. Med. Chem. 2012, 55, 5121−5129

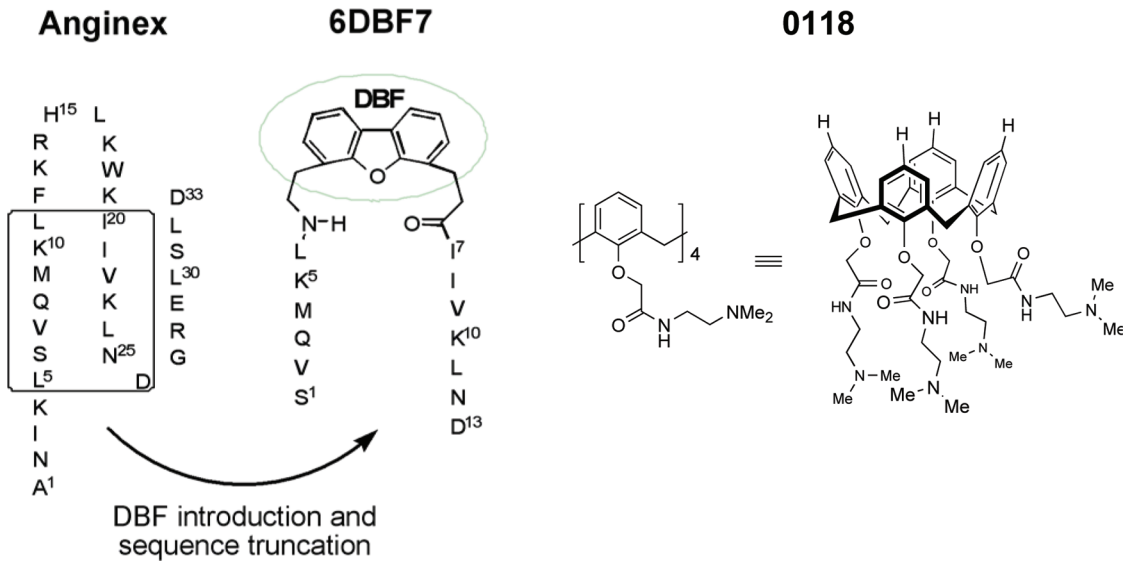

Figure 1. The amino acid sequence of the antiangiogenic peptide 33mer Anginex is shown, along with the dibenzofuran (DBF)-based mimetic 6DBF7. As described in the text, partial peptide mimetic 6DBF7 was further reduced to a nonpeptidic calix[4]arene-based compound 0118, whose chemical structure is shown in two representations.

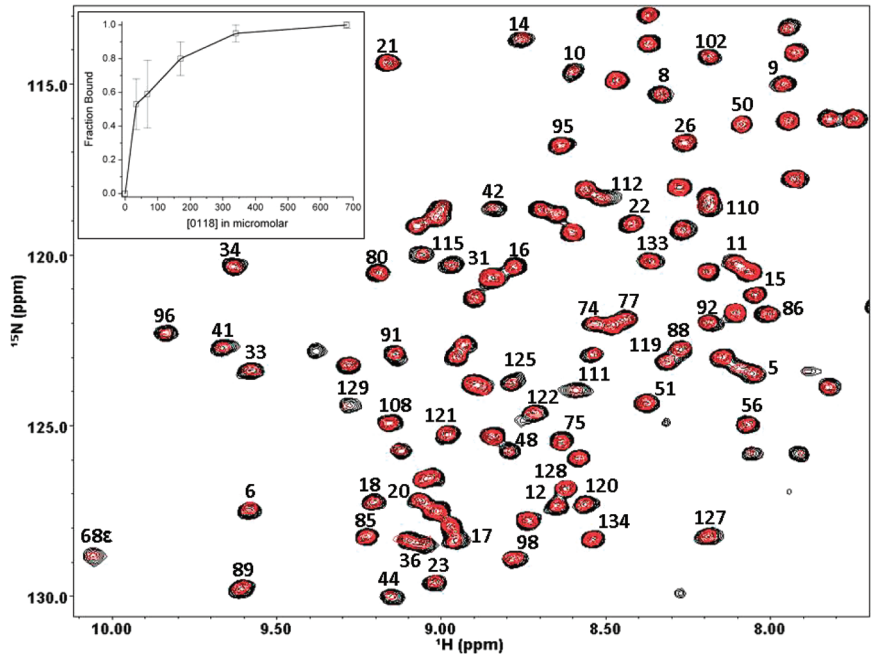

Figure 2. An overlay of two ^{1}H−^{15}N HSQC spectral expansions are shown for ^{15}N-enriched gal-1 (1 mg/mL) alone (cross peaks in black) and in the presence of 400 μM 0118 (cross peaks in red). Resonances are labeled with assignments reported previously by Nesmelova et al.[30] The insert shows the concentration of unbound or free 0118 ligand calculated by subtracting the estimated fraction bound of 0118 from the total concentration of 0118 added to the solution.

present study, we used NMR spectroscopy to demonstrate that galectin-1 is in fact a molecular target of calixarene 0118 and, furthermore, that 0118 interacts with this lectin at a site other than its carbohydrate binding site. We also report here that 0118 attenuates galectin-1 binding to cell surface glycans and galectin-1-mediated cell agglutination and that it inhibits cell proliferation in a dose-dependent manner that is correlated with the expression of galectin-1 in cells in culture. Overall, this work contributes to the clinical development of the promising galectin-1-targeting agent 0118.

RESULTS

Figure 2 shows an overlay of two ^{15}N−^{1}H HSQC NMR spectra of uniformly ^{15}N-labeled galectin-1 (^{15}N-gal-1), one in the absence (cross-peaks in black) and one in the presence (cross-peaks in red) of 400 μM 0118. While some resonances are not perturbed by the presence of 0118, others are differentially reduced in intensity (apparent resonance broadening) and chemically shifted. This observation alone indicates that 0118 interacts with gal-1. Moreover, these NMR spectral effects demonstrate that the binding exchange between 0118 and gal-1 occurs on the intermediate chemical shift time scale.[20]

dx.doi.org/10.1021/jm300014q | J. Med. Chem. 2012, 55, 5121−5129

Although one can not generally determine an accurate equilibrium ligand dissociation constant, K_d, from these data, a plot of 0118-induced intensity changes averaged over all resonances vs the concentration of 0118 does yield a saturable binding curve (insert Figure 2). Here, we have actually plotted the concentration of unbound or free 0118 ligand calculated by subtracting the estimated fraction bound of 0118 from the total concentration of 0118 added to the solution, e.g., the total concentration of 0118 at 50% was 60 μM, and because the total gal-1 monomer concentration was 60 μM, 30 μM would be bound. In this instance, there would be also 30 μM 0118 free in solution as plotted. This midpoint value of 30 μM, therefore, is a reasonable estimate of the K_d value and is consistent with the observation that 0118 binding to gal-1 occurs in the intermediate exchange regime on the NMR chemical shift time scale, where the equilibrium dissociation constant, K_d, for ligand binding should fall in the range of ~5−100 μM. Ligand binding with a K_d value greater than ~100 μM would be observed as fast exchange on the chemical shift time, whereas a K_d value less than ~1 μM would be observed as slow exchange on the chemical shift time scale.[20] Note that these ranges are only approximate.

Because the 0118-gal-1 binding event falls in the intermediate exchange regime, Figure 3A shows a resonance broadening map[21] in which differential broadening is shown relative to resonance intensities for the gal-1 free state. Fractional changes are calculated by subtracting from 1 the intensity of a given HSQC cross-peak divided by that in pure gal-1 at the same protein concentration. A value of 1 indicates that a resonance is no longer apparent, and a value of 0 indicates no change in resonance intensity. Although the degree of resonance broadening depends on several factors, including the strength of ligand binding and chemical shift differences between unbound and bound states, a resonance broadening map developed at the initial stages of the ligand titration provides relatively good insight into where on the protein the ligand interacts. In this regard, the interpretation of an HSQC broadening map is similar to that of the well-known HSQC chemical shift map,[22] i.e., those resonances that are broadened the most are associated with that site(s) of interaction on gal-1. However, because resonances in the intermediate exchange regime are chemically shifted as they are broadened (some more than others) and this is correlated with the chemical shift difference between bound and unbound states, we also show a HSQC chemical shift map in Figure 3B, also taken at the same initial point in the titration before resonances are too highly broadened and disappear from the spectrum.

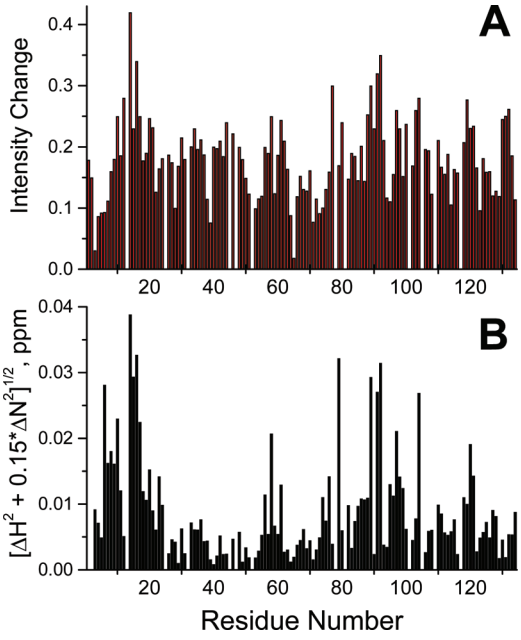

Figure 3. HSQC resonance broadening (A) and chemical shift (B) maps are shown for 0118 binding to gal-1. Fractional changes in gal-1 resonance intensities observed for gal-1 in the presence of 0118 (170 μM) are shown vs the residue number of gal-1 (A). A value of 1 indicates that the resonance associated with that particular residue is no longer apparent, and a value of zero indicates no change in resonance intensity. Chemical shift changes to ^{15}N-gal-1 resonances in the presence of 0118 are shown vs the residue number of gal-1 (B).

Both broadening and chemical shift maps show similar trends and essentially indicate which gal-1 residues are primarily affected by 0118 binding, and therefore, they indicate the region on gal-1 where 0118 is most likely to interact (Figure 4). Gal-1 has a β-sandwich structure that is comprised of 11 β-strands, with the front face β-sheet (antiparallel running β-strands 1, 3, 10, 4, 5, and 6) containing the lactose binding site and the back face β-sheet comprising β-strands 7, 8, 9, 2, and 11. β-strands 1 and 11 interact to form the gal-1 dimer interface. From our HSQC resonance broadening and chemical shift maps (Figure 3), we conclude that the primary site for 0118 interaction is at the back face of gal-1 in the region formed primarily by residues 6−10, 14−17, and 89−92. Other residues also perturbed by 0118 binding are mostly proximal to these residues. For example, L17 is proximal to M120, and F91 is proximal to T97 which is proximal to Y104.

The region identified above is highlighted (circle in left panel of Figure 4), along with some other proximal residues, in one of the monomer subunits of the gal-1 dimer (PDB access code 1gzw). The chemical structure of 0118 is shown to scale in the insert at the bottom of the figure. The panel at the right in Figure 4 shows the front face of gal-1 with bound lactose in blue, and the middle panel shows a side view where it is apparent that most perturbations are observed at residues on the back side of gal-1. Nevertheless, by perturbing this network of residues at the back face of gal-1, 0118 binding consequently perturbs residues at the front face of gal-1 where carbohydrate ligands bind. In this regard, residues N56, I58, and N61, along with E74 and V76, are indirectly perturbed by 0118 binding. This may be explained by considering that Y104 is proximal to E74 and V76 which lie above the carbohydrate ligand, while I89 is proximal to N61 through the β-sandwich. Moreover, M120 is proximal to F79, which interacts with I58, also within the hydrophobic interior of the β-sandwich. In other words, it appears that when 0118 binds at the back face of the β-sandwich, effects are seen at the front face carbohydrate binding site.

It should be noted that the side chains of N56 and N61 form hydrogen bonds with OH groups from the carbohydrate ligand,[23] and 0118 binding-induced perturbations to these (and other) residues likely would have influence on carbohydrate ligand binding. In fact, we find that lactose binding to gal-1 is attenuated in the presence of 0118. Figure 5 shows ^{15}N-gal-1 (100 μM) HSQC-derived lactose binding curves acquired in the absence and presence of 0118 (gal-1:0118 molar ratio of 1:5). For each of the four residues shown (S29, N39, R73, and F79), curves acquired with gal-1 in the presence of 0118

dx.doi.org/10.1021/jm300014q | J. Med. Chem. 2012, 55, 5121−5129

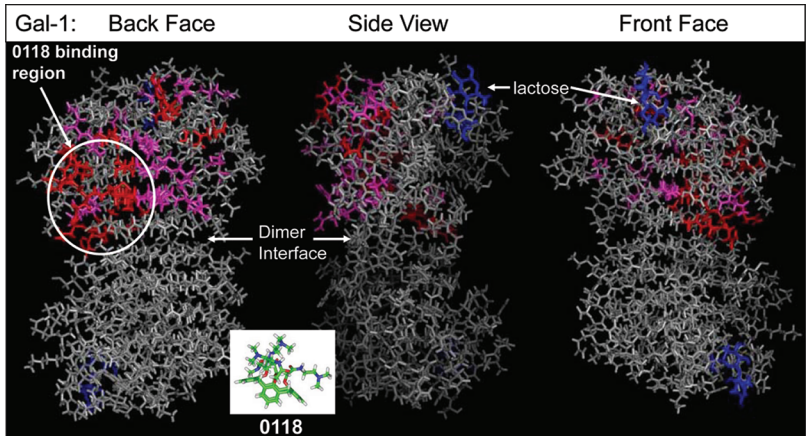

Figure 4. The dimer structure of gal-1 (PDB access code 1gzw) is shown. Residues that are most broadened and chemically shifted as indicated in Figure 2 are highlighted here. The most perturbed resonances are highlighted in red, followed by pink, and those minimally perturbed and unaffected are shown in gray highlights. The proposed 0118 binding region on gal-1 is indicated by a white circle. Three faces are depicted: the lactose (in blue) binding front face, the back side opposite the lactose binding face, and a side view between the two faces looking on edge through the β-sandwich. A stick structure of 0118 is shown to scale in the insert at the bottom of the figure.

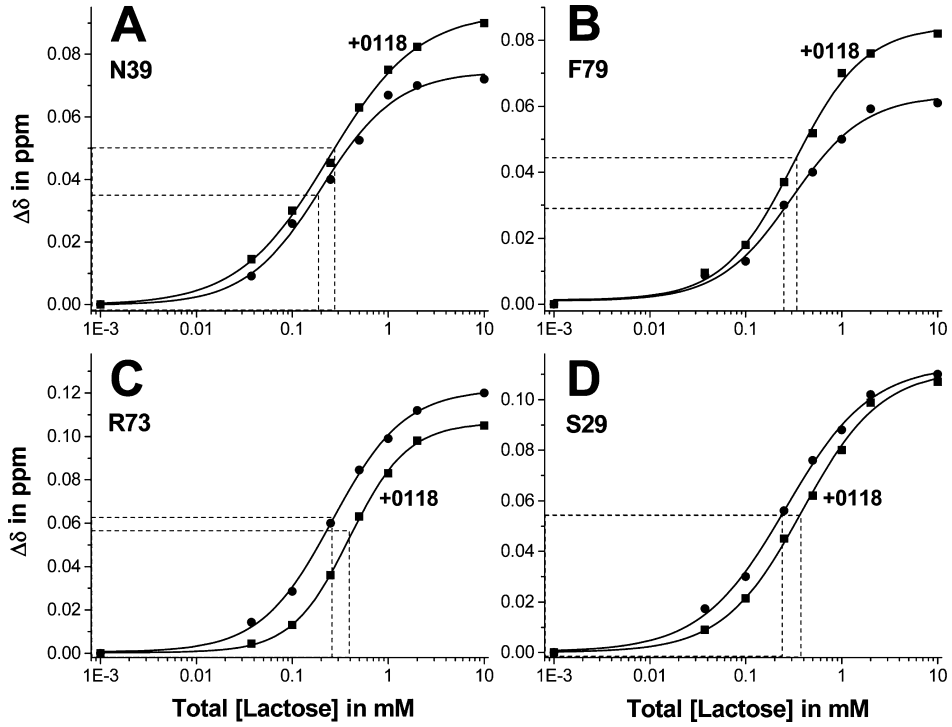

Figure 5. Lactose titration curves for four gal-1 residues (S29, N39, R73, and F79) are shown. $^{1}H,^{15}N$-weighted chemical shift differences ($\Delta\delta = [(\delta^{1}H)^2 + 0.15(\delta^{15}N)^2]^{1/2}$) were determined from HSQC spectra acquired with ^{15}N-gal-1 (100 μM) in the absence (−●−) and presence of 0118 (−■−) in a molar ratio of 1:5 (gal-1:0118). The total lactose concentration is shown in these plots. Titration curves were fit with Gaussian/sigmoidal functions, and K_d values were determined by taking the total lactose concentration at 50% $\Delta\delta$ minus the concentration of bound lactose (i.e., half of the gal-1 concentration = 50 μM).

(compared to those in the absence of 0118) are shifted to higher concentrations of lactose, indicating weaker ligand binding to the lectin. While the average K_d value for binding of lactose to Gal-1 is 100 ± 40 μM in the absence of 0118, it is 290 ± 55 μM in the presence of 0118. These K_d values are the result of averaging of individual K_d values determined for the 20 top lactose-induced gal-1 shifted resonances.

0118-induced attenuation of carbohydrate (lactose) binding to gal-1 is supported on the cellular level by three lines of evidence. First, results from flow cytometry indicate that FITC-labeled gal-1 (0.1 μM or 0.2 μM) binding to natural glycans on splenocytes is significantly attenuated as the concentration of 0118 is increased (Figure 6A). The effect is deconvoluted with respect to leukocytes ($CD4^+$ and $CD8^+$ cells) and endothelial cells ($CD31^+$) in Figure 6B. In these cell types, 0118 effectively attenuates binding of FITC-gal-1 to cell surface glycans in a dose-dependent manner. At 20 μM 0118, binding of 0.1 μM gal-1 to $CD4^+$ (or $CD8^+$) and $CD31^+$ cells is ~80% and ~50% inhibited, respectively. At 100 μM 0118, gal-1 binding to $CD4^+$ (or $CD8^+$) and $CD31^+$ cells is 100% and ~70% inhibited, respectively. In this regard, gal-1 binding is inhibited in a dose-dependent manner, i.e., a higher concentration of 0118 is

dx.doi.org/10.1021/jm300014q | J. Med. Chem. 2012, 55, 5121−5129

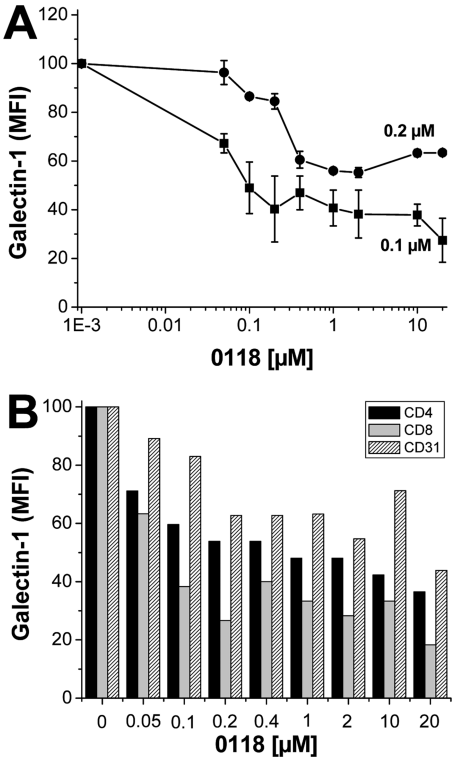

Figure 6. Multicolor flow cytometry was used to assess the effects of 0118 on FITC-gal-1 binding to splenocytes (CD4+ and CD8+ leukocytes and CD31+ endothelial cells) derived from male or female gal-1 −/− null mice. Binding of FITC-gal-1 (0.1 or 0.2 μM) to these cells was assessed as a function of 0118 concentration. Experiments were performed on a LSR II flow cytometer (BD Biosciences), and data were analyzed using Flowjo software (Tree Star, Inc.).

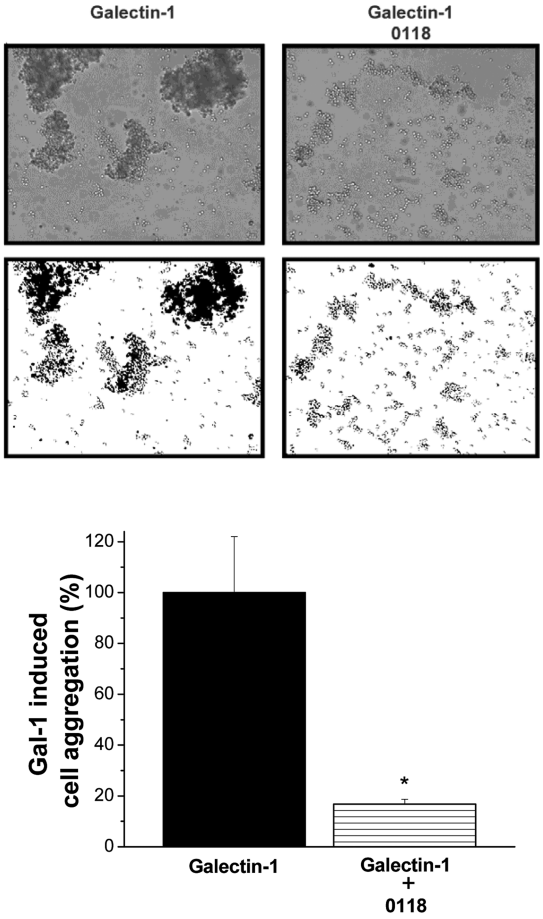

Figure 7. Jurkat E6.1 cells agglutination was induced by addition of 1 μM gal-1 and incubated at 22 °C on plastic, round-bottom chamber slides (Nunc, Naperville, IL, USA) in medium alone or in the presence of 20 μM 0118. Cell agglutination was assessed using an Axiovert 10 inverted phase microscope equipped with a digital camera system (Zeiss, Germany) and digitally analyzed and differentially quantified by morphometric analysis, as described earlier.[25]

required to inhibit the binding of gal-1 to cell surface glycans when the lectin concentration is 0.2 μM vis-à-vis 0.1 μM.

Our second line of evidence that carbohydrate binding to gal-1 is attenuated by 0118 binding comes from the agglutination assay (Figure 7). Because agglutination occurs by galectin-1-mediated cross-linking of cell surface glycans on cells,[24] attenuated agglutination in the presence of 0118 can be explained by reduced glycan binding by 0118-bound gal-1. At a gal-1 concentration that induces ∼50% cell agglutination (1 μM), Figure 7A (panels at the left) shows formation of large aggregates as expected in the absence of 0118. Upon addition of 0118 (20 μM) (panels at the right in Figure 7A), it is evident that agglutination is highly attenuated. These data were digitally quantified by pixilation,[25] as illustrated in the lower panels to Figure 7A. These results are presented in bar graph format in Figure 7B, which indicates that the presence of 0118 at 20 μM inhibits cell agglutination by about 80%.

The concentration responsiveness from 0118 in these flow cytometry and agglutination experiments with gal-1 parallels that observed in a cell viability assay using a series of human cell lines that express varying amounts of gal-1. Figure 8A shows the dose-dependent 0118 inhibition on several cell types in culture, and Figure 8B quantifies these results for gal-1 protein production relative to that of β-actin as a control. Figure 8C shows a scatter plot correlating the IC_{50} values for 0118 with the amount of mRNA gal-1 (*LGALS1*) expressed in each of those cancer cells. The correlation coefficient (R = 0.55, p-value = 0.002) is reasonably good, with an inverse correlation indicating that concentrations of 0118 required to inhibit 50% of cancer cell growth is proportional to *LGALS1* expression. Although we can not rule out the possibility that 0118 also exerts its effect on cell viability distinct from its effect on gal-1, the major mechanism of action from 0118 is most likely to be via inhibition of gal-1 function, primarily because we do observe a correlation between the level of gal-1 expression and the effectiveness of 0118, i.e. more gal-1 expression requires more 0118 to achieve the same biological response. Nevertheless, 0118 could also be functioning via an additional mechanism of action.

■ DISCUSSION

Here, we report that calixarene compound 0118 indeed targets gal-1. 0118 was designed as a topomimetic of the amphipathic, angiogstatic peptide Anginex.[12a] Over the past several years, our approach to designing mimetics of Anginex has reduced the size and peptidic character of the parent peptide 33mer to a dibenzofuran-based partial peptide mimetic, 6DBF7[12b] and then to calixarene compound 0118.[15] Previously, we demonstrated that all three compounds (Anginex, 6DBF7, and 0118) function similarly in vitro and in vivo in terms of, e.g., inhibiting endothelial cell proliferation, angiogenesis, and tumor growth.[12a,27]

dx.doi.org/10.1021/jm300014q | J. Med. Chem. 2012, 55, 5121−5129

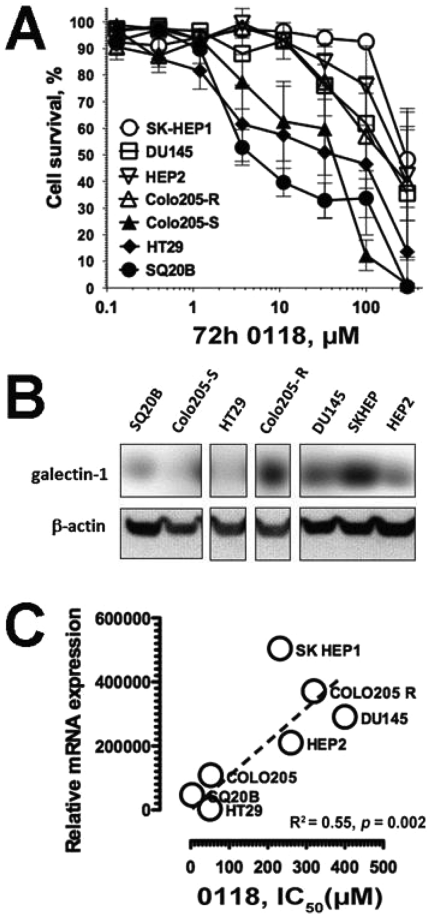

Figure 8. The concentration of 0118 required for inhibiting cell viability is proportional to Gal-1 expression. (A) Antiviability effects (expressed as % change in cell numbers over time) of 0118 were determined using the MTT assay in human cancer cell lines. (B) Cancer cells that are sensitive to 0118 expressed lower galectin-1 protein expression as determined using Western Blot analysis. (C) Concentrations of 0118 as established by plotting the IC_{50} in cancer cells is proportional to their relative *LGALS1* mRNA expression as assessed by qRT-PCR.

However, although the structures of all three compounds are similar in terms of, e.g., being amphipathic and cationic, the actual structural presentation of chemical groups in 0118 is quite different from that in Anginex or 6DBF7. The hydrophobic surface of β-sheet-folded Anginex (and 6DBF7) is composed of aromatic (Phe and Trp) and alkyl (Leu, Val, Ile) groups, whereas its hydrophilic, cationic surface is primarily composed of primary amines (Lys). Chemical substituents on the hydrophobic and hydrophilic surfaces of 0118 are composed solely of aryl groups and tertiary amines, respectively. Nevertheless, on the molecular level, there must be sufficient chemical similarity between Anginex (and 6DBF7) and 0118 in order to promote 0118 targeting to gal-1 as with Anginex.[14]

The greater difference between the chemical surfaces of Anginex and 0118 rests in the character of their cationic faces (primary vs tertiary amines, respectively). However, SAR information on Anginex indicates that it is the hydrophobic face of the amphipathic peptide that interacts with the surface of gal-1, while the cationic face of Anginex primarily promotes longer range electrostatic effects.[12b] In this regard, it may be that the hydrophobic surface from the calixarene crown of 0118 is also more crucial to interaction with gal-1. This idea is consistent with our HSQC mapping data that suggest that the most likely 0118 binding site has considerable hydrophobic character defined by e.g. P13, G14, A94, F91, L112, L114, and A116, as well as anionic character with, e.g., E15, D92, and E115.

As an antagonist of gal-1, calixarene 0118 is unique to the field, primarily because it binds at a site on gal-1 that is located on the back face of the lectin away from its β-galactoside-binding site. Moreover, our HSQC-based lactose titrations, as well as flow cytometry and agglutination data, indicate that 0118 attenuates binding of gal-1 to lactose and to cell surface glycans. Because of this and the observation that 0118 binds gal-1 at a site different from its carbohydrate binding site, we conclude that 0118 functions as a noncompetitive, allosteric inhibitor of gal-1 function, unlike any other known galectin antagonist.

Galectin antagonists reported to date are mostly β-galactoside-analogues and glycomimetics that target the obvious, canonical carbohydrate binding site. Most of these compounds were designed to antagonize galectins 1, 3, 7, 8, and 9 (primarily gal-3) and include aryl *O*- and *S*-galactosides and lactosides,[8a,28] carbohydrate-based triazoles and isoxazoles,[28] 3-(1,2,3-triazol-1-yl)-1-thio-galactosides,[8b] anomeric oxime ether derivatives of β-galactose (*O*-galactosyl aldoximes),[9] phenyl thio-β-D-galactopyranoside analogues,[8d] thioureido *N*-acetyllactosamine derivatives,[8c] and multivalent arene thiodigalactoside bis-benzamido analogues with groups on each end of the carbohydrate moiety to interact with arginine residues within the carbohydrate binding domain.[8e] Other multivalent inhibitors include functionalized unnatural amino acids (phenyl-bis-alanine and phenyl-tris-alanine) with 2-azidoethyl β-D-galactopyranosyl-(1−4)-β-D-glucopyranoside,[10] a bilactosylated steroid-based compound,[29] and polymethylene-spaced dilactoseamine derivatives.[11]

Although some of these carbohydrate-based compounds bind various galectins in vitro with single digit μM K_d values, most bind galectins rather weakly with K_ds >100 μM. Moreover, galectin specificity of any of them remains a significant issue, due primarily to conserved structural homology of β-galactoside binding sites among all galectins. In addition, few of these compounds has been tested in vivo, where issues related to bioavailabilty are likely to show that these saccharide-based compounds would make for relatively poor therapeutic agents, primarily because simple, low molecular weight carbohydrates are readily subject to hydrolysis and/or clearance.

■ CONCLUSION

0118 has been developed as a therapeutic agent for use in the clinic against cancer. As a therapeutic agent, calixarene 0118 is a significant improvement over both Anginex and 6DBF7, as well as over any carbohydrate-based compound, for several reasons. 0118 (937 Da) approaches the generally accepted definition of a "small molecule" (i.e., < 500 Da). 0118 should have better in vivo exposure because it is nonpeptidic and noncarbohydrate, and therefore is nonhydrolyzable. Moreover, because of its aryl-crown structure, 0118 should be chemically stable and less likely to be metabolized in vivo than any peptide or carbohydrate-based compound. Compound 0118 is presently in a phase I clinical trial with cancer patients. Overall, 0118 is a promising antitumor agent that targets galectin-1 as a first-in-class therapeutic agent.

dx.doi.org/10.1021/jm300014q | J. Med. Chem. 2012, 55, 5121−5129

MATERIALS AND METHODS

Chemicals. Calix[4]arene 0118 (PTX008; PepTx, Excelsior MN; USA) is also known as OTX-008 (OncoEthix, Lausanne; Switzerland) was manufactured as previously described.[15] Purity of 0118 is >95% as determined by chromatography and mass spectrometry, as described elsewhere.[15]

Galectin-1 Preparation. "Uniformly ^{15}N-labeled human galectin-1 (gal-1) was expressed in BL21(DE3) competent cells (Novagen), grown in minimal media, purified over a B lactose affinity column, and further fractionated on a gel filtration column, as described previously by Nesmelova et al.[30] Typically, 44 mg of purified protein were obtained from 1 L of cell culture. The purity of the final sample was quantified by using the Biorad protein assay and was checked for purity by using SDS PAGE. Functional activity of the purified protein was assessed by a T-cell death assay."[30]

FITC-Galectin-1 Preparation. Gal-1 was conjugated with fluorescein isothiocyanate (FITC) using a FITC:protein molar ratio of 10:1. Gal-1 (2 mg/mL) was dissolved in 500 μM of 20 mM potassium phosphate buffer, pH 7.4, followed by addition of ~50 μL of FITC (10 mg/mL) that had been dissolved in 0.1 mM sodium bicarbonate. The resulting lower pH (~pH 8) ensured selective labeling at the N-terminal amine group of the protein.[31] This solution was then mixed thoroughly and incubated at room temperature (22 °C) for 18 h in the dark. During the course of the reaction, the mixture was gently vortexed 3 or 4 times. The resulting FITC-labeled protein was separated from unbound dye by filtration using an Amicon Ultra cellulose filter (Millipore, 10 kDa cutoff). MALDI-TOF MS demonstrated the addition of the 389 Da FITC label to galectin-1 and suggested >90% labeling efficiency.

Heteronuclear NMR Spectroscopy. "Uniformly ^{15}N-labeled recombinant gal-1 was dissolved at a concentration of 1 mg/mL in 20 mM potassium phosphate buffer at pH 7.0, 50 μM EDTA, made up using a 95% H_2O/5% D_2O mixture. ^{1}H−^{15}N HSQC NMR experiments were used to investigate binding of 0118 to ^{15}N-labeled gal-1. ^{1}H and ^{15}N resonance assignments for gal-1 were previously reported."[30,32]

"NMR experiments were carried out at 30 °C on a Varian Unity Inova 600-MHz spectrometer equipped with an H/C/N triple-resonance probe and $x/y/z$ triple-axis pulse field gradient unit. A gradient sensitivity-enhanced version of two-dimensional ^{1}H−^{15}N HSQC was applied with 256 ($t1$) × 2048 ($t2$) complex data points in nitrogen and proton dimensions, respectively."[30] Raw data were processed by using NMRPipe[33] and were analyzed by using NMRview.[34]

Flow Cytometry. Male and female gal-1 null mice (Jackson Laboratory) were provided water and standard chow ad libitum and were maintained on a 12-h light/dark cycle prior to experiments that were approved by the University of Minnesota Research Animal Resources Ethical Committee. For FACS experiments, spleens from these mice (6−10 weeks old) were harvested and nonenzymatically disrupted by shear force to yield single-cell suspensions.[16] Cell suspensions were prepared in Hanks's balanced solution. Red blood cells were lysed in ACK (Lonza Walkersville) for 5 min on ice, and suspensions were filtered through nylon mesh. Spleen cells were then washed and incubated with monoclonal antibodies as indicated for 40 min on ice. After an additional washing step, various concentrations of gal-1 (with or without 0118) were added and incubated for 30 min on ice. Prior to FACS analysis, cell suspensions were washed once more and analyzed by multiparameter flow cytometry on a LSR II flow cytometer (BD Biosciences) using Flowjo software (Tree Star, Inc.).[16]

Agglutination Assay. Jurkat E6.1 cells (2 × 10^6/200 μL RPMI 1640 medium) agglutination was induced by 1 μM gal-1 and were incubated on plastic round-bottom chamber slides (Nunc, Naperville, IL, USA) in medium alone or with 20 μM 0118 at 22 °C. Subsequently, the cells were analyzed for agglutination with an Axiovert 10 inverted phase microscope equipped with a digital camera system (Zeiss, Germany) and digitally analyzed and differentially quantified by morphometric analysis, as described earlier.[25]

Cell Lines. HEP2, SQ20B, HT29, DU145, and SKHEP1 cells were obtained from the ATCC (Rockville, Maryland, USA). COLO205-S cells were obtained from the National Cancer Institute collection. The COLO205-R cell line was developed from COLO205 cells with resistance to ingenol-3-angelate protein kinase C modulator and displayed cross-resistance to enzastaurin (LY317615-HCl, Eli Lily).[26,35] Cells were grown as monolayers in RPMI medium supplemented with 10% fetal calf serum (Invitrogen, Cergy-Pontoise, France), 2 mM glutamine, 100 units/mL penicillin, and 100 μg/mL streptomycin at 37 °C in a humidified 5% CO_2 atm and regularly checked for the absence of Mycoplasma.

Cell Viability Assay. Cell viability (i.e., cell proliferation and/or cytotoxicity) was determined using the MTT assay (3-[4,5-dimethylthiazol-2-yl]-2,5-diphenyltetrazolium bromide; Sigma, Saint-Quentin Fallavier, France). The conversion of yellow water-soluble tetrazolium MTT into purple insoluble formazan is catalyzed by mitochondrial dehydrogenases and used to estimate the number of viable cells. In brief, cells were seeded in 96-well tissue culture plates at a density of 2 × 10^3 cells/well. After 72 h drug exposure and a 48 h wash-out period, cells were incubated with 0.4 mg/mL MTT for 4 h at 37 °C. After incubation, the supernatant was discarded, insoluble formazan precipitates were dissolved in 0.1 mL of DMSO, and the absorbance was measured at 560 nm by use of a microplate reader (Thermo, France). Wells with untreated cells or with drug-containing medium without cells were used as positive and negative controls, respectively. IC_{50} was determined as half the maximal inhibitory drug concentration for each cell line.

Real-Time Reverse Transcriptase PCR (RT-PCR). The theoretical and practical aspects of real-time quantitative RT-PCR using the ABI Prism 7900 sequence detection system (Perkin-Elmer Applied Biosystems, Foster City, California, USA) have been described in detail elsewhere.[36] Results were expressed as n-fold differences in target gene expression relative to the TBP gene (an endogenous RNA control) and relative to a calibrator (1× sample), consisting of the cell line sample from our tested series with the smallest amount of target gene mRNA. Experiments were performed in duplicate.

Western Blot Analysis. Cells were lysed in buffer containing 50 mM HEPES (pH 7.6), 150 mM NaCl, 1% Triton X-100, 2 mM sodium vanadate, 100 mM NaF, and 0.4 mg/mL phenylmethylsulfonyl fluoride. Equal amounts of protein (30 μg/lane) were subjected to SDS-PAGE and transferred to nitrocellulose membranes. Membranes were blocked with 5% milk in 0.05% Tween 20/phosphate-buffered saline (PBS) and incubated with the primary antibody overnight. Membranes were then washed and incubated with the secondary antibody conjugated to horseradish peroxidase. Bands were visualized using the enhanced chemiluminescence Western blotting detection system. Densitometric analysis was performed under conditions that yielded a linear response. The polyclonal antigalectin-1 antibodies were purchased from Abcam, Paris, France, and generated as described.[18,37] All antibodies were used at a 1:1000 dilution.

AUTHOR INFORMATION

Corresponding Author

*Phone: 001-612-625-9968. E-mail: mayox001@umn.edu.

Author Contributions

⊥R.P.M.D. and M.C.M. contributed equally to work presented in this manuscript.

Notes

The authors declare the following competing financial interest(s): KHM has equity in PepTx, a company that has licensed 0118 from the University of Minnesota.

ACKNOWLEDGMENTS

This work has been supported by a research grant from the National Cancer Institute (NIH R01 CA096090) to K.H.M. M.C.M. was supported by the Cancer Biology Training Grant to the University of Minnesota from the National Institutes of

Health (NIH T32 CA009138). NMR instrumentation was provided with funds from the National Science Foundation (BIR-961477), the University of Minnesota Medical School, and the Minnesota Medical Foundation. E.R., L.A.-X. and M.S. were supported by OncoEthix, the Foundation Nelia & Amadeo Barleta (FNAB), and the Association pour la Recherche & l'Enseignement en Cancérologie (AAREC). We are most grateful and indebted to Prof. Linda Baum and Mabel Pang of the Department of Pathology and Laboratory Medicine, UCLA, for providing us with their expression system (vector/plasmid) for human gal-1.

■ ABBREVIATIONS USED

gal-1, galectin-1; CRD, carbohydrate recognition domain; NMR, nuclear magnetic resonance; HSQC, heteronuclear single quantum coherence; calixarene 0118 (aka PTX008 or OTX008)

■ REFERENCES

(1) Barondes, S. H.; Castronovo, V.; Cooper, D. N.; Cummings, R. D.; Drickamer, K.; Feizi, T.; Gitt, M. A.; Hirabayashi, J.; Hughes, C.; Kasai, K.; et al. Galectins: a family of animal beta-galactoside-binding lectins. *Cell* **1994**, *76* (4), 597−598.

(2) Liu, F. T.; Rabinovich, G. A. Galectins as modulators of tumour progression. *Nature Rev. Cancer* **2005**, *5* (1), 29−41.

(3) Neri, D.; Bicknell, R. Tumour vascular targeting. *Nature Rev. Cancer* **2005**, *5* (6), 436−46.

(4) Perillo, N. L.; Pace, K. E.; Seilhamer, J. J.; Baum, L. G. Apoptosis of T cells mediated by galectin-1. *Nature* **1995**, *378* (6558), 736−739.

(5) Fischer, C.; Sanchez-Ruderisch, H.; Welzel, M.; Wiedenmann, B.; Sakai, T.; Andre, S.; Gabius, H. J.; Khachigian, L.; Detjen, K. M.; Rosewicz, S. Galectin-1 interacts with the {alpha}5{beta}1 fibronectin receptor to restrict carcinoma cell growth via induction of p21 and p27. *J. Biol. Chem.* **2005**, *280* (44), 37266−37277.

(6) Yang, R. Y.; Rabinovich, G. A.; Liu, F. T. Galectins: structure, function and therapeutic potential. *Expert Rev. Mol. Med.* **2008**, *10*, e17.

(7) Ingrassia, L.; Camby, I.; Lefranc, F.; Mathieu, V.; Nshimyumukiza, P.; Darro, F.; Kiss, R. Anti-galectin compounds as potential anti-cancer drugs. *Curr. Med. Chem.* **2006**, *13* (29), 3513−3527.

(8) (a) Sirois, S.; Giguere, D.; Roy, R. A first QSAR model for galectin-3 glycomimetic inhibitors based on 3D docked structures. *Med. Chem.* **2006**, *2* (5), 481−489. (b) Salameh, B. A.; Leffler, H.; Nilsson, U. J. 3-(1,2,3-Triazol-1-yl)-1-thio-galactosides as small, efficient, and hydrolytically stable inhibitors of galectin-3. *Bioorg. Med. Chem. Lett.* **2005**, *15* (14), 3344−3346. (c) Salameh, B. A.; Sundin, A.; Leffler, H.; Nilsson, U. J. Thioureido *N*-acetyllactosamine derivatives as potent galectin-7 and 9N inhibitors. *Bioorg. Med. Chem.* **2006**, *14* (4), 1215−1220. (d) Cumpstey, I.; Carlsson, S.; Leffler, H.; Nilsson, U. J. Synthesis of a phenyl thio-beta-D-galactopyranoside library from 1,5-difluoro-2,4-dinitrobenzene: discovery of efficient and selective monosaccharide inhibitors of galectin-7. *Org. Biomol. Chem.* **2005**, *3* (10), 1922−1932. (e) Cumpstey, I.; Sundin, A.; Leffler, H.; Nilsson, U. J. *C*2-Symmetrical thiodigalactoside bis-benzamido derivatives as high-affinity inhibitors of galectin-3: efficient lectin inhibition through double arginine−arene interactions. *Angew. Chem., Int. Ed. Engl.* **2005**, *44* (32), 5110−5112.

(9) Tejler, J.; Leffler, H.; Nilsson, U. J. Synthesis of *O*-galactosyl aldoximes as potent LacNAc-mimetic galectin-3 inhibitors. *Bioorg. Med. Chem. Lett.* **2005**, *15* (9), 2343−2345.

(10) Tejler, J.; Tullberg, E.; Frejd, T.; Leffler, H.; Nilsson, U. J. Synthesis of multivalent lactose derivatives by 1,3-dipolar cycloadditions: selective galectin-1 inhibition. *Carbohydr. Res.* **2006**, *341* (10), 1353−1362.

(11) Rabinovich, G. A.; Cumashi, A.; Bianco, G. A.; Ciavardelli, D.; Iurisci, I.; D'Egidio, M.; Piccolo, E.; Tinari, N.; Nifantiev, N.; Iacobelli, S. Synthetic lactulose amines: novel class of anticancer agents that induce tumor-cell apoptosis and inhibit galectin-mediated homotypic cell aggregation and endothelial cell morphogenesis. *Glycobiology* **2006**, *16* (3), 210−220.

(12) (a) Dings, R. P.; Mayo, K. H. A journey in structure-based drug discovery: from designed peptides to protein surface topomimetics as antibiotic and antiangiogenic agents. *Acc. Chem. Res.* **2007**, *40* (10), 1057−1065. (b) Mayo, K. H.; Dings, R. P.; Flader, C.; Nesmelova, I.; Hargittai, B.; van der Schaft, D. W.; van Eijk, L. I.; Walek, D.; Haseman, J.; Hoye, T. R.; Griffioen, A. W. Design of a partial peptide mimetic of anginex with antiangiogenic and anticancer activity. *J. Biol. Chem.* **2003**, *278* (46), 45746−45752. (c) Dings, R. P.; van der Schaft, D. W.; Hargittai, B.; Haseman, J.; Griffioen, A. W.; Mayo, K. H. Anti-tumor activity of the novel angiogenesis inhibitor anginex. *Cancer Lett.* **2003**, *194* (1), 55−66.

(13) Dings, R. P.; Williams, B. W.; Song, C. W.; Griffioen, A. W.; Mayo, K. H.; Griffin, R. J. Anginex synergizes with radiation therapy to inhibit tumor growth by radiosensitizing endothelial cells. *Int. J. Cancer* **2005**, *115* (2), 312−319.

(14) Thijssen, V. L.; Postel, R.; Brandwijk, R. J.; Dings, R. P.; Nesmelova, I.; Satijn, S.; Verhofstad, N.; Nakabeppu, Y.; Baum, L. G.; Bakkers, J.; Mayo, K. H.; Poirier, F.; Griffioen, A. W. Galectin-1 is essential in tumor angiogenesis and is a target for antiangiogenesis therapy. *Proc. Natl. Acad. Sci. U.S.A.* **2006**, *103* (43), 15975−15980.

(15) Dings, R. P.; Chen, X.; Hellebrekers, D. M.; van Eijk, L. I.; Zhang, Y.; Hoye, T. R.; Griffioen, A. W.; Mayo, K. H. Design of nonpeptidic topomimetics of antiangiogenic proteins with antitumor activities. *J. Natl. Cancer Inst.* **2006**, *98* (13), 932−936.

(16) Dings, R. P.; Vang, K. B.; Castermans, K.; Popescu, F.; Zhang, Y.; Oude Egbrink, M. G.; Mescher, M. F.; Farrar, M. A.; Griffioen, A. W.; Mayo, K. H. Enhancement of T-cell-mediated antitumor response: angiostatic adjuvant to immunotherapy against cancer. *Clin. Cancer Res.* **2011**, *17* (10), 3134−3145.

(17) (a) van der Schaft, D. W.; Dings, R. P.; de Lussanet, Q. G.; van Eijk, L. I.; Nap, A. W.; Beets-Tan, R. G.; Bouma-Ter Steege, J. C.; Wagstaff, J.; Mayo, K. H.; Griffioen, A. W. The designer anti-angiogenic peptide anginex targets tumor endothelial cells and inhibits tumor growth in animal models. *FASEB J.* **2002**, *16* (14), 1991−1993. (b) Dings, R. P.; Yokoyama, Y.; Ramakrishnan, S.; Griffioen, A. W.; Mayo, K. H. The designed angiostatic peptide anginex synergistically improves chemotherapy and antiangiogenesis therapy with Angiostatin. *Cancer Res.* **2003**, *63* (2), 382−385. (c) Dings, R. P.; Loren, M.; Heun, H.; McNiel, E.; Griffioen, A. W.; Mayo, K. H.; Griffin, R. J. Scheduling of radiation with angiogenesis inhibitors Anginex and Avastin improves therapeutic outcome via vessel normalization. *Clin. Cancer Res.* **2007**, *13* (11), 3395−3402.

(18) Rubinstein, N.; Alvarez, M.; Zwirner, N. W.; Toscano, M. A.; Ilarregui, J. M.; Bravo, A.; Mordoh, J.; Fainboim, L.; Podhajcer, O. L.; Rabinovich, G. A. Targeted inhibition of galectin-1 gene expression in tumor cells results in heightened T cell-mediated rejection: a potential mechanism of tumor-immune privilege. *Cancer Cell* **2004**, *5* (3), 241−251.

(19) Lotan, R.; Matsushita, Y.; Ohannesian, D.; Carralero, D.; Ota, D. M.; Cleary, K. R.; Nicolson, G. L.; Irimura, T. Lactose-binding lectin expression in human colorectal carcinomas. Relation to tumor progression. *Carbohydr. Res.* **1991**, *213*, 47−57.

(20) Keeler, J. *Understanding NMR Spectroscopy*; John Wiley & Sons: Chichester, West Sussex, England; Etobicoke, Ontario, Canada, 2005; p xv, 459 pp.

(21) Miller, M. C.; Klyosov, A.; Mayo, K. H. The α-galactomannan Davanat binds galectin-1 at a site different from the conventional galectin carbohydrate binding domain. *Glycobiology* **2009**, *19* (9), 1034−1045.

(22) Rajagopal, P.; Waygood, E. B.; Reizer, J.; Saier, M. H., Jr.; Klevit, R. E. Demonstration of protein−protein interaction specificity by NMR chemical shift mapping. *Protein Sci.* **1997**, *6* (12), 2624−2627.

(23) Lopez-Lucendo, M. F.; Solis, D.; Andre, S.; Hirabayashi, J.; Kasai, K.; Kaltner, H.; Gabius, H. J.; Romero, A. Growth-regulatory human galectin-1: crystallographic characterisation of the structural

changes induced by single-site mutations and their impact on the thermodynamics of ligand binding. *J. Mol. Biol.* **2004**, *343* (4), 957−970.

(24) Levroney, E. L.; Aguilar, H. C.; Fulcher, J. A.; Kohatsu, L.; Pace, K. E.; Pang, M.; Gurney, K. B.; Baum, L. G.; Lee, B. Novel innate immune functions for galectin-1: galectin-1 inhibits cell fusion by Nipah virus envelope glycoproteins and augments dendritic cell secretion of proinflammatory cytokines. *J. Immunol.* **2005**, *175* (1), 413−420.

(25) (a) Dings, R. P.; Van Laar, E. S.; Webber, J.; Zhang, Y.; Griffin, R. J.; Waters, S. J.; MacDonald, J. R.; Mayo, K. H. Ovarian tumor growth regression using a combination of vascular targeting agents anginex or topomimetic 0118 and the chemotherapeutic irofulven. *Cancer Lett.* **2008**, *265* (2), 270−280. (b) Dings, R. P.; Van Laar, E. S.; Loren, M.; Webber, J.; Zhang, Y.; Waters, S. J.; Macdonald, J. R.; Mayo, K. H. Inhibiting tumor growth by targeting tumor vasculature with galectin-1 antagonist anginex conjugated to the cytotoxic acylfulvene, 6-hydroxylpropylacylfulvene. *Bioconjugate Chem.* **2010**, *21* (1), 20−27.

(26) Serova, M.; Astorgues-Xerri, L.; Bieche, I.; Albert, S.; Vidaud, M.; Benhadji, K. A.; Emami, S.; Vidaud, D.; Hammel, P.; Theou-Anton, N.; Gespach, C.; Faivre, S.; Raymond, E. Epithelial-to-mesenchymal transition and oncogenic Ras expression in resistance to the protein kinase Cbeta inhibitor enzastaurin in colon cancer cells. *Mol. Cancer Ther.* **2010**, *9* (5), 1308−1317.

(27) Dings, R. P.; Arroyo, M. M.; Lockwood, N. A.; Van Eijk, L. I.; Haseman, J. R.; Griffioen, A. W.; Mayo, K. H. Beta-sheet is the bioactive conformation of the anti-angiogenic anginex peptide. *Biochem. J.* **2003**, *23*, 281−288.

(28) Giguere, D.; Sato, S.; St-Pierre, C.; Sirois, S.; Roy, R. Aryl *O*- and *S*-galactosides and lactosides as specific inhibitors of human galectins-1 and -3: role of electrostatic potential at O-3. *Bioorg. Med. Chem. Lett.* **2006**, *16* (6), 1668−1672.

(29) Ingrassia, L.; Nshimyumukiza, P.; Dewelle, J.; Lefranc, F.; Wlodarczak, L.; Thomas, S.; Dielie, G.; Chiron, C.; Zedde, C.; Tisnes, P.; van Soest, R.; Braekman, J. C.; Darro, F.; Kiss, R. A lactosylated steroid contributes in vivo therapeutic benefits in experimental models of mouse lymphoma and human glioblastoma. *J. Med. Chem.* **2006**, *49* (5), 1800−1807.

(30) Nesmelova, I. V.; Pang, M.; Baum, L. G.; Mayo, K. H. ^{1}H, ^{13}C, and ^{15}N backbone and side-chain chemical shift assignments for the 29 kDa human galectin-1 protein dimer. *Biomol. NMR Assignments* **2008**, *2* (2), 203−205.

(31) (a) Hungerford, G.; Benesch, J.; Mano, J. F.; Reis, R. L. Effect of the labelling ratio on the photophysics of fluorescein isothiocyanate (FITC) conjugated to bovine serum albumin. *Photochem. Photobiol. Sci.* **2007**, *6* (2), 152−158. (b) Hermanson, G. T., *Bioconjugate Techniques*, 2nd ed.; Academic Press: Burlington, MA, 2008; Part *1*, 1202 pp.

(32) Nesmelova, I. V.; Dings, R. P. M.; Mayo, K. H., Understanding galectin structure−function relationships to design effective antagonists. In *Galectins*; Klyosov, A. A., Witczak, Z. J., Platt, D., Eds.; John Wiley & Sons: Hoboken, NJ, 2008; pp 33−69.

(33) Delaglio, F.; Grzesiek, S.; Vuister, G. W.; Zhu, G.; Pfeifer, J.; Bax, A. NMRPipe: a multidimensional spectral processing system based on UNIX pipes. *J. Biomol. NMR* **1995**, *6* (3), 277−293.

(34) Johnson, B. A. Using NMRView to visualize and analyze the NMR spectra of macromolecules. *Methods Mol. Biol.* **2004**, *278*, 313−352.

(35) Ghoul, A.; Serova, M.; Astorgues-Xerri, L.; Bieche, I.; Bousquet, G.; Varna, M.; Vidaud, M.; Phillips, E.; Weill, S.; Benhadji, K. A.; Lokiec, F.; Cvitkovic, E.; Faivre, S.; Raymond, E. Epithelial-to-mesenchymal transition and resistance to ingenol 3-angelate, a novel protein kinase C modulator, in colon cancer cells. *Cancer Res.* **2009**, *69* (10), 4260−4269.

(36) Bieche, I.; Parfait, B.; Laurendeau, I.; Girault, I.; Vidaud, M.; Lidereau, R. Quantification of estrogen receptor alpha and beta expression in sporadic breast cancer. *Oncogene* **2001**, *20* (56), 8109−8115.

(37) Juszczynski, P.; Ouyang, J.; Monti, S.; Rodig, S. J.; Takeyama, K.; Abramson, J.; Chen, W.; Kutok, J. L.; Rabinovich, G. A.; Shipp, M. A. The AP1-dependent secretion of galectin-1 by Reed Sternberg cells fosters immune privilege in classical Hodgkin lymphoma. *Proc. Natl. Acad. Sci. U.S.A.* **2007**, *104* (32), 13134−13139.